Quantification the filling of microcracks due to Autogenous self-healing in cement paste

Chen, Jiayi; Liu, Xian; Ye, Guang

Publication date
2016

Document Version
Final published version

Published in
Proceedings of the International RILEM Conference Materials, Systems and Structures in Civil Engineering 2016

Citation (APA)
Chen, J., Liu, X., & Ye, G. (2016). Quantification the filling of microcracks due to Autogenous self-healing in cement paste. In M. Azenha, I. Gabrijel, D. Schlicke, T. Kanstad, & O. Mejlhede Jensen (Eds.), *Proceedings of the International RILEM Conference Materials, Systems and Structures in Civil Engineering 2016: Segment on Service Life of Cement-Based Materials and Structures* (PRO 109 ed., Vol. 2, pp. 745-754). Article 76 RILEM Publications S.A.R.L..

International RILEM Conference on Materials, Systems and Structures in Civil Engineering
Conference segment on Service Life of Cement-Based Materials and Structures
22-24 August 2016, Technical University of Denmark, Lyngby, Denmark

QUANTIFICATION THE FILLING OF MICROCRACKS DUE TO AUTOGENOUS SELF-HEALING IN CEMENT PASTE

Jiayi Chen [(1)], Xian Liu [(2)], Guang Ye [(1)]

(1) Delft University of Technology, Delft, The Netherlands
(2) Tongji University, Shanghai, China

Abstract
Microcracks play vital roles in the prediction of the service life of concrete structure. Because microcracks in concrete structure are the preferential ingression channels for aggressive ions, e.g., chloride, sulphate, etc. However, microcracks have potentials to self-heal autogenously due to the continuous hydration of unhydrated cement, especially when ultra-/ high strength concrete is used. To quantify the autogenous self-healing effects of microcracks in cement paste, our experiment is designed to monitor the self-healing process of microcracks in cement paste continuously by using optical microscope. The healing products are quantified by image analysis with newly implemented software in MATLAB. The results indicate that the microcracks are not filled evenly along the crack length and most healing products are $Ca(OH)_2$, which dissolve partly from the paste matrix and re-nucleate in the microcrack, in addition to its counterpart from the continuous hydration of unhydrated cement. Furthermore, the sample cracked at earlier age shows higher potential to heal, while the sample with smaller crack width experiences greater filling efficiency. The obtained autogenous self-healing mechanism will be used in the future simulation.

1. Introduction

Microcracks (crack width below 0.1mm) are inevitable in concrete structure, especially when high thermal stresses happen in mass concrete members. Microcracks play vital roles in the prediction of the service life of concrete structure. Because they are the preferential ingression channels for ingressive ions, e.g., chloride, sulphate, etc. For instance, the chloride migration coefficients of concrete samples with microcracks caused by rapid freezing and thawing cycles experienced 2.5 to 8 times higher than that the references [1]. Fortunately, microcracks have the potentials to self-heal due to the continuous hydration of unhydrated cement, especially for ultra-/high strength concrete. Abrams [2] observed that the compressive

strength of the specimens recovered: the specimens had been tested first at 28 days, then the cracked specimens were stored outdoors and exposed to the weather for eight years before the compressive strength was measured again. The recovered strength was more than twice of the 28 day strength after 8 years [2]. However, many researchers pointed out that the recoveries of mechanical properties are less significant compared to the recoveries of transport properties and the continuity of the sample [1-3]. While the mechanical properties of concrete with microcracks recovered less than 10% after self-healing under water for 3 months at 20℃, the chloride migration coefficient reduced between 25% and 40%, and the ultrasonic pulse velocity (UPV) recovered from 50% to 100% [1]. The 40% reduced chloride migration coefficient indicates that the cracks are partly filled. The UPV recovery of 100% shows the crack space is bridged, so the continuity of the sample is rebuilt. Therefore, it can be assumed that the autogenous self-healing only happens at a few places where the microcracks are partly or completely blocked by newly formed hydration products. To confirm the assumption and to evaluate the efficiency of autogenous self-healing of the microcracks, an experimental process is designed to monitor the self-healing process of microcracks in cement paste, by which the amount of healing products are quantified.

2. Materials and methods

In this study, optical microscope is used to continuously monitor the autogenous self-healing process. Under optical microscope the water can remain in liquid form at room temperature. The reaction conditions for further hydration are similar to that in reality. The thin section sample is prepared with thickness of 100 μm. As a result, it becomes possible to distinguish the cracking space, origin paste matrix and newly formed hydration product under an optical microscope. With the polarized filters in the optical microscope, the qualification analysis can be carried out.
The general experiment process is explained as follows: the experiment started with casting cement paste samples in sealed plastic cylindrical containers with different water to cement (w/c) ratios, followed by curing them at 20 ℃. At desired ages, the samples were ground to 100 μm in thickness and cracked under microscope to specified crack widths. At last the samples were saturated with water and sealed, so the self-healing process was monitored. The specific procedures will be demonstrated in section 2.2.

2.1 Materials

In this study, Portland cement CEM I 42.5N is used. The sample series are shown in table 1. Various variables are presented, including w/c ratios, curing ages before cracking, and the average crack widths. All samples are monitored under optical microscope for 3 days after cracking.

2.2 Methods

2.2.1 Preparation of thin section samples

At the desired age, the cement paste samples were removed from the plastic containers. The samples were cut to 1 cm in thickness for thin section machine. SiC Paper is a type of coated abrasive that consists of sheets of paper with abrasive material glued to one face. Prior to gluing the sample with the working glass, SiC Paper #120 grits was used to sand one surface

in order to increase the contact area. Another surface of the sample was ground and polished to 1000±10 μm in thickness. This finished surface was glued to the object glass with acetone-dissoluble glue. Afterwards, the sample was turned over and cut again to make a new working surface. Similarly, this surface was ground and polished until the thickness of the sample is 100±10 μm. The thin section sample was ready for next procedure.

Table 1 Sample series

	w/c ratio	Age (day)	Crack width (μm)		w/c ratio	Age (day)	Crack width (μm)
A25S07W40	0.25	7	40	A25S28W80	0.25	28	80
A50S07W40	0.5	7	40	A50S28W80	0.5	28	80
A25S28W40	0.25	28	40	A25S07W120	0.25	7	120
A50S28W40	0.5	28	40	A50S07W120	0.5	7	120
A25S07W80	0.25	7	80	A25S28W120	0.25	28	120
A50S07W80	0.5	7	80	A50S28W120	0.5	28	120

2.2.2 Cracking samples under optical microscope

In order to generate the microcracks in samples many approaches were reported: 1) Microcracks were distributed randomly in the sample after rapid freezing and thawing cycles [1-4]. 2) The crack-width controlled splitting test to gain the microcracks [5-8]. 3) Huang et al obtained the microcracks of 30 μm by attaching two ground and polished samples to each other [9].For the first approach, the crack width obtained from rapid freezing and thawing cycles ranges from 1 to 10 μm; however, this range is too narrow for systematic studies of the microcracks. The second and third approaches generate artificial cracks with two characteristic shapes, i.e., V shape and flat shape, respectively. The real microcracking pattern cannot be represented by these two methods.

In this research, a new pre-crack technique was proposed to obtain specific crack width in a more realistic shape. Several steps are followed: firstly, the thin section sample was immerged in acetone solution to dissolve the glue combined the sample with the object glass. Secondly, the thin section sample was rinsed carefully with ethanol and dried in the air. Thirdly, the sample was bended and cracked into two parts, of which one part was glued again with a new object glass. Fourthly, another part of the cracked sample was placed close to the newly crack flank and adjusted subtly under the optical microscope. This part was glued to keep the crack in place when the specific crack width was measured under the optical microscope. The mode of the optical microscope is LEITZ DMRXP 301-371.010.

2.2.3 Petrographic analysis

The petrographic analysis uses the polarising and scanning electron microscopes to obtain information about the mineralogy, compositional features, etc.[10]. When the light from the bottom source goes through a polarized filter, the light is polarized at one direction. As the light goes through the thin section sample, the crystal phases reflect the light into other directions, i.e., non-polarized. Another polarized filter is used perpendicular to the first one,

so the light is polarized again. These two polarized filters are called crossed polarized filters, by this, only the crystal phases are shown in the images; therefore the amorphous calcium silicate hydrates (C-S-H) phase are not included in further analysis. From this way the general phase information of the hydration products were obtained.

2.2.4 Monitoring under optical microscope

When the micro-cracked sample was ready, the double-side tape was glued around the sample. After being saturated in water, the sample was covered with covering glass. The covering glass was sealed along the edges with transparent nail polish, to avoid the air leakage and the water evaporation; therefore the paste matrix will not be carbonated during the experiment.

The sample was then monitored under the optical microscope with the external callipers at x and y directions to control the movement of sample. A computer was connected with the optical microscope to take photos in each 30 minutes. Both images under the polarized filter and under the crossed polarized filters were taken. To improve the experiment efficiency, three different samples were placed under the optical microscope to obtain images in each 30 minutes. The total monitoring time was 3 days. The images obtained for one sample were used to conduct the image analysis with newly implemented MATLAB software.

2.2.5 Image analysis

The disturbance in the images was happened when the samples were changed regularly during the observation under optical microscope. The images could shift in x and y directions and rotation in x-y panel. As shown in Figure 1, the analysis software was implemented in MATLAB. The software could relocate the images back to their original locations, i.e., removing the disturbance in terms of the shifts in x and y directions and rotation in x-y panel. Afterwards, the images were used for further image analysis.

In Figure 1, on the left top of the Graphical User Interface (GUI), the image called origin image is the first image taken during the experiment. On the left bottom the image called target image is subjected to relocation. The image on the right in Figure 1 is the superimposed image of origin and target images to show the differences.

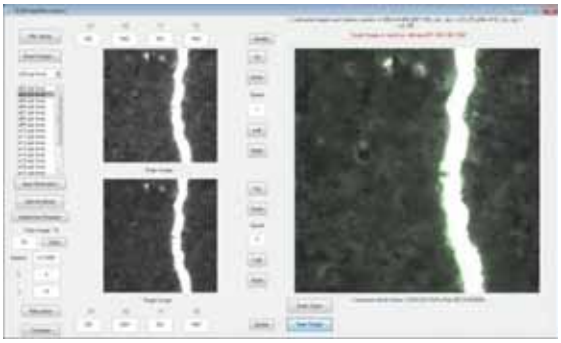

Figure 1. GUI of the analysis software

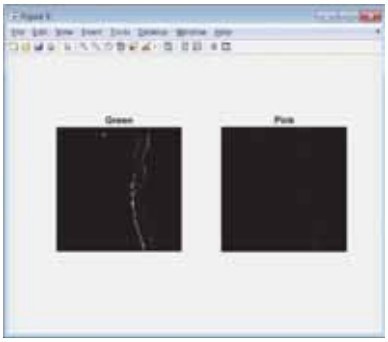

Figure 2. Example of relocation result

2.2.5.1 Relocation operation

Because the rotation centre (o_x, o_y), dx and dy (shifts in x and y direction) are 4 unknown variables, 4 points from the origin image and the counterpart points from the target image are chosen. Consequently, the rotation angle and shifts of dx and dy can be calculated. The values can be manually changed if the relocation result is not optimized.

In Figure 2, the pixels belonging to target image rather than origin image are shown on the left, which represent the hydration products. The pixels belonging to origin image rather than target image are shown on the right. These pixels are the errors that should be eliminated as much as possible. After being carefully adjusted, the amount of these pixels is reduced to less than 0.05% of total amount of pixels.

2.2.5.2 Analysis procedure

In order to quantify the hydration products, during image processing only the hydration products and the crack space are selected, other pixels are removed completely after the relocation operation.

Figure 3 gives an example of the intermediate images during the analysis. These images demonstrate the procedure how the hydration products and the crack space are selected. Firstly, the target image in Figure 3(a) is filtered with grayscale threshold, generating the crack mask given in Figure 3(b). Secondly, the crack area in Figure 3(c) is cut out from the target image with the aid of crack mask. Lastly, the hydration products are selected from the crack area with the help of grayscale threshold. From the crack mask, the crack widths are calculated along the crack from top to bottom. Similarly, the hydration products are quantified. The filling rate is calculated along the crack from top to bottom as shown in Figure 4(a). The filling rate is sorted and then grouped according to the filling efficiency, e.g., 0%, from 0% to 10%, etc. The statistical analysis is given in Figure 4(b). The x axis is the filling efficiency, the columns are the length of locations with these filling efficiencies divided by the total length of the crack in percentage (left y axis) and the curve is the cumulative curve of analysed locations in percentage (right y axis).

4. Results and discussion

The analysis results of samples with different w/c ratios, curing ages and average crack widths are compared.

4.1 Influence of w/c ratios

To demonstrate the influences of different w/c ratios on self-healing, sample A25S28W40 with w/c of 0.25 and sample A50S28W40 with w/c of 0.50 are compared. As shown in Figure 5(b), about 25% length of crack in sample A25S28W40 does not show any change in terms of crack widths. It indicates that no hydration products are formed within the crack space. 20% the length of crack is filled up to 5%, i.e., the crack width at these locations decreases by 5%.

Similarly, the filling efficiencies for the rest of the crack are shown in Figure 5(b). In sample A25S28W40, the highest filling efficiency is about 35%. In other words, there is a significant decrease in crack width at some locations.

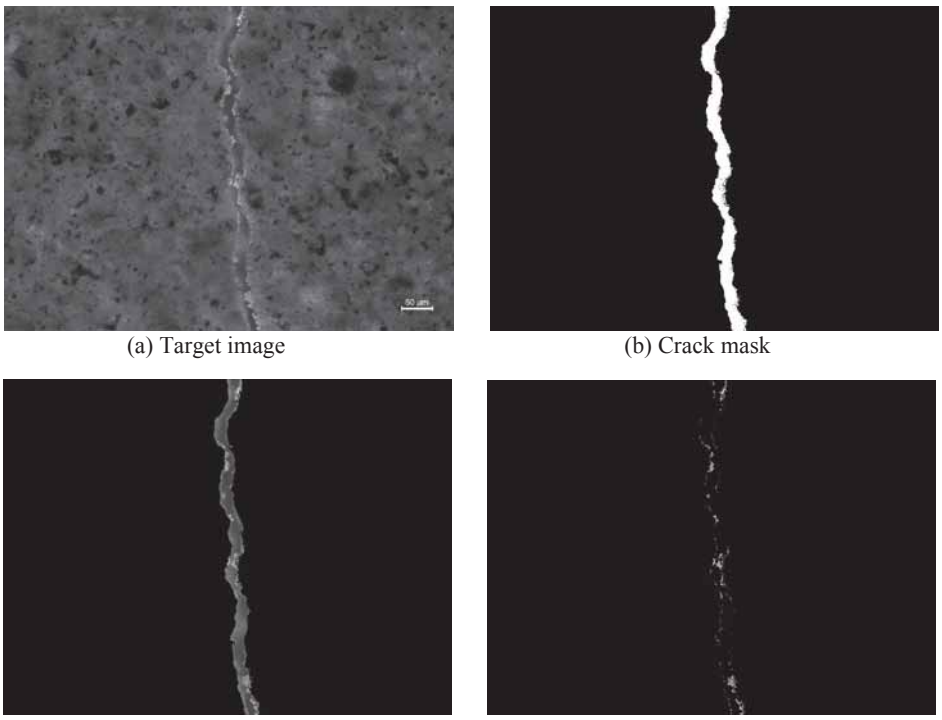

(a) Target image (b) Crack mask

(c) Crack area (d) Hydration product

Figure 3. Analysis of hydration products and crack space

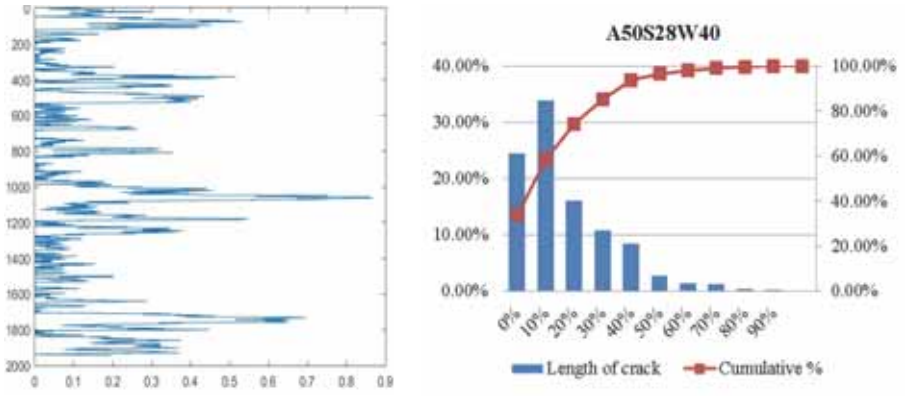

(a) Filling rate along the crack (b) Statistical analysis

Figure 4. Filling rate and statistical analysis

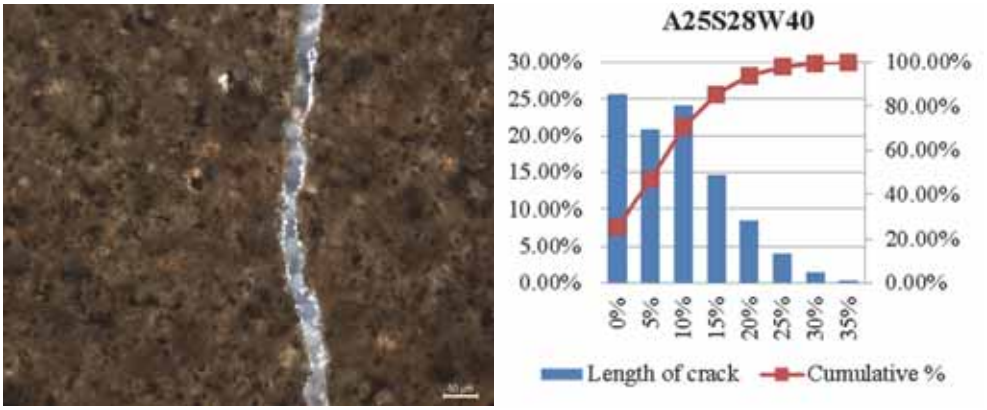

(a) Final image (b) Filling effiency

Figure 5. Quantification of hydration products in A25S28W40 after self-healing for 3 days

For A50S28W40 shown in Figure 6, about 25% the length of crack exhibits no filling effect at all. The filling efficiencies for the 35.49% length of the crack are between 20% and 40%. The rest 6.17% length of the crack is filled from 50% to 90%.

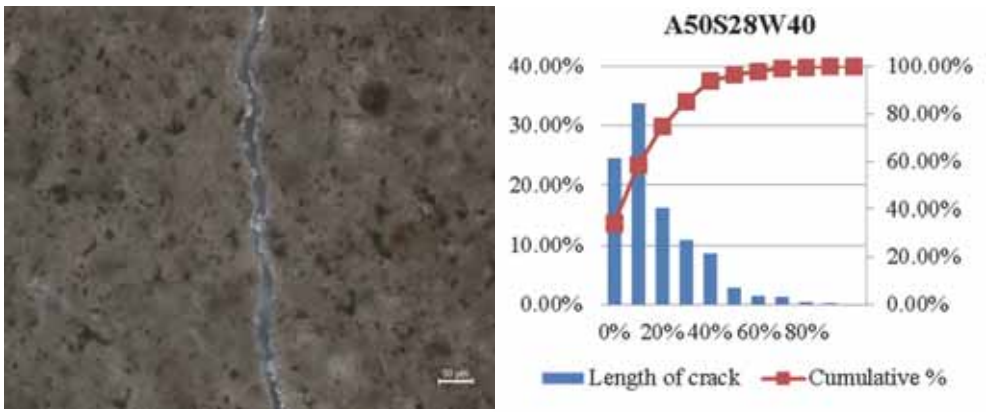

(a) Final image (b) Filling efficiency

Figure 6. Quantification of hydration products in A50S28W40 after self-healing for 3 days

It was expected that the sample with lower w/c ratios would have a higher filling efficiency due to higher amount of unhydrated cement available for further hydration. Surprisingly, the A50S28W40 with higher w/c shows much better filling effect in general. The reason is probably attributed to the dissolution of existing hydration products from the matrix of cement paste. Lauer and Slate also reported that cement phase with a higher w/c ratio experienced better healing effects, and they proposed that when the calcium hydroxide was

used during the reaction within the crack space, more calcium hydroxide ions diffused from the interior, i.e., the paste matrix [11]. This phenomenon can explain why A50S28W40 have a higher filling efficiency than A20S28W40. Furthermore, it suggests that long-term autogenous self-healing is possible even after the cement particles are completely hydrated, as long as the water is present.

Notably, the greatest filling efficiency of 90% in A50S28W40 is of significance: if the crack were the path for transporting ions, the 0.31% length of the crack in A50S28W40 would not be noticeable in terms of length, however it would be the "critical neck" in the overall transporting process. In other words, the autogenous self-healing contributes to better transport properties by partially blocking the microcracks. Further investigation is need to study the influences of the blocking of microcracks on the transport properties due to autogenous self-healing.

4.2 Influence of curing ages before cracking samples

Similarly, healing efficiency of A25S28W40 and A25S07W40, as shown in Figure 5 and Figure 7, are compared with respect to different curing ages, i.e., 28 days and 7 days before cracking.

About 25% of the length of crack in A25S28W40 with 28 days curing does not have any filling effect. The percent of the length of crack without healing in A25S07W40 with 7 days curing is less than 15%, and the greatest filling efficiency is about 80%. It is indicated that samples with micro-cracks at early age have a higher potential to heal themselves. A possible explanation for this might be that the samples with microcracks at early age have higher amount of unhydrated cement particles exposed to or near to the crack edge.

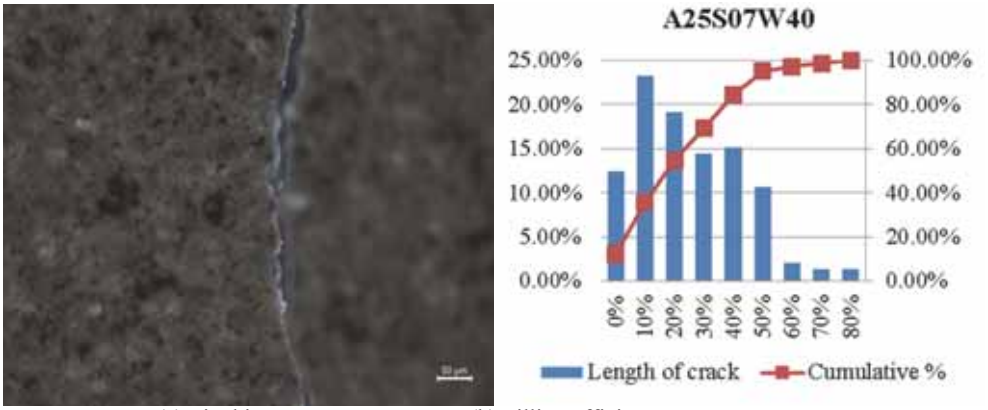

(a) Final image (b) Filling efficiency

Figure 7. Quantification of hydration products in A25S07W40 after self-healing for 3 days

However, it should be noticed that the experiments were carried out under the conditions avoiding any moisture and air exchanging. The carbonation is prevented explicitly. The contribution of the carbonation during the healing process is not taken into account in this

study. A general petrographic analysis was carried out to qualify the hydration products. The results from petrographic analysis indicate that most healing products within the crack space are calcium hydroxide. Neville claimed that the autogenous self-healing phenomena were attributed principally to further hydration of unhydrated cementitious materials based on his early results [12]. However, it was explained later by him that this was only applicable to young concrete, and the predominant products in the crack space was calcium carbonate [13]. Additionally, It was reported that the maximum chloride diffusivities of samples from field were more than 10 times lower than those obtained from the same concrete under laboratory condition [14]. The self-healing effect is greatly underestimated under the laboratory condition. To fully understand the influences of the self-healing on concrete with microcracks, the impacts of carbonation should be taken into account.

4.3 Influence of average crack widths

Samples with average crack widths of 40 μm (A25S07W40) and 80 μm (A25S07W80) are compared. It is observed from Figure 7 and Figure 8 that two samples show similar distributions in terms of the right-skewed shapes. This distribution shape indicates that the amount of hydration products is limited by the nature of the w/c ratio and the age before cracking [15]. It can therefore be assumed that the amount of hydration products is similar for these two samples, so the filling efficiency is only affected by the crack width. Specifically, the lengths of crack without any hydration products are 12.46% and 19.60% for A25S07W40 and A25S07W80, respectively. The crack width of 25S07W80 is twice that of the A25S07W40, and the former has almost double the length of crack without healing compared to latter. This finding suggests that in general the crack width does not influence the quantity of self-healing products, and the filling efficiency decreases with the increase of crack width.

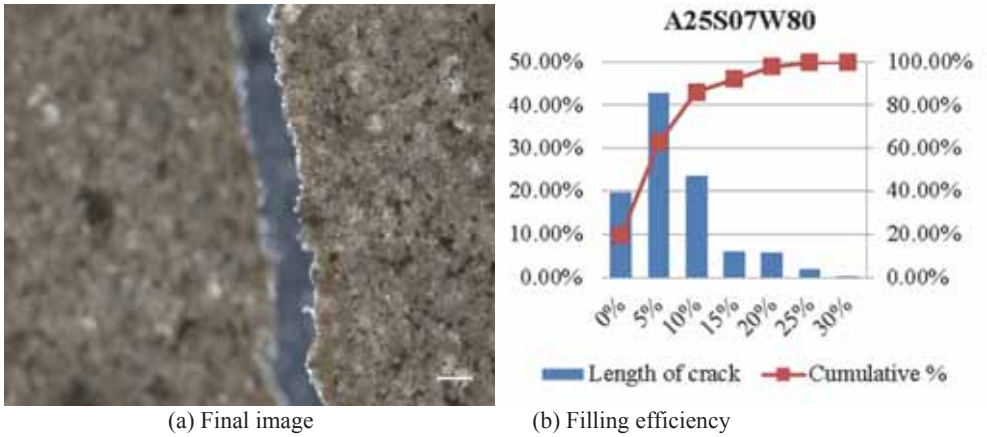

(a) Final image (b) Filling efficiency

Figure 8. Quantification of hydration products in A25S07W80 after self-healing for 3 days

5. Conclusions

In this study the autogenous self-healing process is monitored quantitatively. The influencing factors on the healing efficiency, i.e., various w/c ratios, curing ages before cracking and average crack widths are compared.

It is found that the microcracks are not filled evenly along the crack path; some locations are blocked to a greater extent than the rest. The sample of higher w/c ratio experiences better filling effect has shown that the hydration products formed in the crack space may be attributed to the dissolution of existing hydration products from the cement paste. The samples cracked at earlier age or with smaller crack widths show high self-healing potential. The presence of water may play vital roles regarding the long-term autogenous self-healing effects even after the cement particles are completely hydrated.

The condition for carbonation is avoided explicitly during the experiments for simplification. Future research should take into account the influences of carbonation on self-healing of concrete, which may further boost the autogenous self-healing effects in the long term.

References

[1] Jacobsen, S., J. Marchand and L. Boisvert, Effect of cracking and healing on chloride transport in OPC concrete, Cement and Concrete Research 26 (1996), 869-881.
[2] Jacobsen, S. and E.J. Sellevold, Self healing of high strength concrete after deterioration by freeze/thaw, Cement and Concrete Research 26 (1996), 55-62.
[3] Zhu, Y., Y. Yang and Y. Yao, Autogenous self-healing of engineered cementitious composites under freeze–thaw cycles, Constr. and Build. Materials 34 (2012), 522-530.
[4] Jacobsen, S., J. Marchand and H. Hornain, Sem observations of the microstructure of frost deteriorated and self-healed concretes, Cem. Concr. Res. 25 (1995), 1781-1790.
[5] Jang, S.Y., B.S. Kim and B.H. Oh, Effect of crack width on chloride diffusion coeffs. of concrete by steady-state migration tests, Cem. Concr. Res. 41 (2011), 9-19.
[6] Picandet, V., A. Khelidj and H. Bellegou, Crack effects on gas and water permeability of concretes, Cement and Concrete Research 39 (2009), 537-547.
[7] Park, S.-S., S.-J. Kwon and S.H. Jung, Analysis technique for chloride penetration in cracked concrete using equivalent diffusion and permeation, Construction and Building Materials 29 (2012), 183-192.
[8] Akhavan, A., S.-M.-H. Shafaatian and F. Rajabipour, Quantifying the effects of crack width, tortuosity, and roughness on water permeability of cracked mortars, Cement and Concrete Research 42 (2012), 313-320.
[9] Huang, H., G. Ye and D. Damidot, Characterization and quantification of self-healing behaviors of microcracks due to further hydration in cement paste, Cement and Concrete Research 52 (2013), 71-81.
Alan, B.P. and S. Ian, Concrete Petrography: A Handbook of Investigative Techniques, Second Edition (2015), 3.
[10] Lauer, R.K. and F.O. Slate, Autogenous Healing of Cement Paste, ACI Journal 52 (1956), 1083-1097.
[11] Neville, A., Properties of Concrete, Fourth Edition (1995), 844.
[12] Neville, A., Autogenous Healing—A Concrete Miracle?, Concr. Int. 24 (2002), 76-82.
[13] Sandberg, P. and L. Tang, Field Study of the Penetration of Chlorides and Other Ions Into a High Quality Concrete Marine Bridge Column, Proceedings of the Third International Conference SP-145 (1994), 557-571.
[14] Nancy, R.T., Typical Histogram Shapes and What They Mean, The Quality Toolbox Second Edition (2004), 292-299.